PCCP

RSC Publishing

PAPER

View Article Online
View Journal | View Issue

Cite this: *Phys. Chem. Chem. Phys.*, 2013, **15**, 5163

Revised conformational assignments and conformational evolution of tyrosine by laser desorption supersonic jet laser spectroscopy†

Yoko Shimozono,[ab] Kohei Yamada,[ab] Shun-ichi Ishiuchi,[ab] Koichi Tsukiyama[c] and Masaaki Fujii*[ab]

Received 10th October 2012,
Accepted 30th January 2013

DOI: 10.1039/c3cp43573c

www.rsc.org/pccp

The number of conformers and their structures of tyrosine are reassigned on the basis of resonance enhanced multiphoton ionization (REMPI), ultraviolet–ultraviolet hole burning (UV–UV HB), infrared (IR) dip spectra, and quantum chemical calculations. From comparison between REMPI and UV–UV HB spectra, it was found that 12 conformers coexist in the supersonic jet. The structures of these conformers are determined by the IR spectra and theoretical calculations. The number of conformers is more than that reported in the previous reports (8 conformers), and is rationalized by the systematic formation of conformers from simpler molecules without substituents, just like evolution. The importance of dipole–dipole interaction between an amino-acid chain and hydroxyl group at the benzene ring was also discussed.

I. Introduction

Flexibility is essential for proteins, and their conformational changes, *i.e.* folding and unfolding, are very important for molecular recognition and enzyme reaction processes.[1] Since each conformation of flexible molecules can be distinguished as isomers in the gas phase, conformational studies of peptides by using gas phase spectroscopy has been widely investigated. The strategy of these studies is a bottom-up approach with amino-acid building blocks. That is, by lengthening chains of peptide one by one, we can investigate how peptide conformations evolve, *i.e.* the process of forming the secondary structure of a protein. For this approach, conformational information of each building block, *i.e.* amino-acid, is indispensable. In particular, the conformation of aromatic amino-acids, phenylalanine (Phe),[2–11] tyrosine (Tyr)[2–4,9,10,12–23] and tryptophan,[24–29] has been investigated since the early days of supersonic jet spectroscopy.

Among the aromatic amino-acids, conformational similarity between Tyr and Phe is expected, because Tyr, *p*-hydroxyphenylalanine, is an analog of Phe. However, the similarity between them has not been discussed in terms of their conformational variety. The first report of an electronic spectrum of Phe by detecting laser induced fluorescence (LIF) was by Levy and co-workers in 1991,[2] and the frequencies of 0–0 transitions of 5 conformers, which were labeled A–E in ascending order, were determined by a saturation technique in the next year.[3] In 2000, resonant multiphoton ionization (REMPI) spectrum, UV–UV hole burning (HB) spectra and IR dip spectra of Phe were measured by Simons and co-workers.[5] In that work, a 0–0 transition of a new conformer was found, which was labeled X, and 6 conformers were discovered totally. By comparing observed IR dip spectra, except conformer E, with theoretical ones, they assigned the structure of each conformer. In 2004, however, the structural assignments of the conformers A and E were revised based on the results of the analyses of the rotational contours of the electronic transitions by themselves.[6] The IR dip spectrum of the conformer E was measured by Ebata and co-workers in 2006, and they assigned the structure of E, which however corresponded to the structure suggested by Simons and co-workers in 2000.[7,8] Ebata and co-workers did not discuss this disagreement, however, the assignment in 2004 is conclusive and the IR dip spectrum of the conformer E reported in 2006 can be explained by the assignment in 2004. Therefore, the assignment by Simons and co-workers in 2004 is a consistent conclusion. The notations of A, B, C, D, E and X is

[a] *Chemical Resources Laboratory, Tokyo Institute of Technology, 4259 Nagatsuta-cho, Midori-ku, Yokohama 226-8503, Japan*
[b] *Department of Electronic Chemistry, Interdisciplinary Graduate School of Science and Engineering, Tokyo Institute of Technology, 4259 Nagatsuta-cho, Midori-ku, Yokohama 226-8502, Japan. E-mail: mfujii@res.titech.ac.jp*
[c] *Department of Chemistry, Faculty of Science, Tokyo University of Science, 1-3 Kagurazaka, Shinjuku-ku, Tokyo 162-8601, Japan*

† Electronic supplementary information (ESI) available. See DOI: 10.1039/c3cp43573c

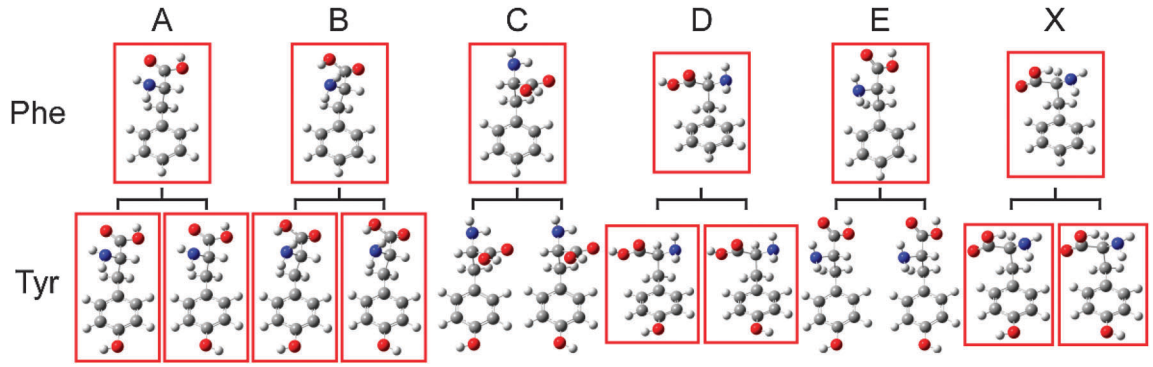

Fig. 1 Expected conformational evolution from phenylalanine to tyrosine. Observed structures are framed by rectangles.

originally the notation of the 0–0 bands of 6 conformers. Hereafter, we use them to discriminate the structures of the 6 conformers (Fig. 1). These 6 conformers arise from different conformations of the amino-acid chain, which can be characterized by the types of intramolecular hydrogen bonds. In the conformer B and X, the carboxyl OH forms a hydrogen bond with a nitrogen atom of an amino group, while other conformers adopt the hydrogen bond between NH and O═C.

For Tyr, 10 conformers were suggested by Levy and co-workers for the first time in 1992 by using the saturation technique.[3] In 2000, de Vries and co-workers reported the REMPI spectrum of Tyr by using a laser desorption source and concluded that Tyr has 8 conformers on the basis of the HB spectroscopy, which however were not presented in the paper.[16] In 2002, the same group revised the number of conformers from 8 to 10 by full analyses of the vibronic bands observed in the REMPI spectrum. Ebata and co-workers reported LIF, HB and IR dip spectra of Tyr in 2007.[19] From the HB spectra, they confirmed the 8 conformers but assigned the rest to the vibronic bands. Here, the S_1 origins of two conformers were interpreted to be overlapped. In 2011, de Vries and co-workers reported REMPI, HB and IR dip spectra, and 0–0 transitions of 8 conformers were identified.[22] Also in this report, the overlap of the S_1 origin of 2 conformers were reported. In the last two reports, the assigned structures are the same, which are given in Fig. 1. However, the correspondence between the 0–0 transition and the structure of each conformer is different (see Table 1).

The 8 conformers can be classified into 4 pairs (see Fig. 1). Two structures in each pair have the same conformation of amino-acid chain and different orientation of the phenolic OH, *i.e.*, relationship between them is rotational isomer (rotamer) with respect to the phenolic OH torsion. This result also means that Tyr has 4 conformations in its amino-acid chain. In addition, these conformations correspond to A, B, D and X of Phe.

As can be seen in the Figure, two conformations of amino-acid chain observed in C and E of Phe are not observed in Tyr. This result implies that there is some interaction between the phenolic OH and the amino-acid chain, and which perturbs conformational stabilities of the amino-acid chain. It is, however, surprising and suspicious because the distance between the phenolic OH and the amino-acid chain is too large to interact strongly. Actually, such interaction is not observed in

Table 1 0–0 Transition energy of each conformer and its assignment

		Conformational assignments		
Conformer	$E(S_1–S_0)/cm^{-1}$	This work	de Vries[a]	Ebata[b]
1	35 491	BS	B	B
2	35 516	AS	A	D
3	35 522	BR	B′	B′
4	35 538	AR	A′	D′
5	35 594	CS	—	—
6	35 608	CR	—	—
7	35 613	XR	X, X′	X, X′
8	35 633	XS	—	—
9	35 641	DR	D	E
10	35 646	DS	D′	E′
11	35 649	IIS	—	—
12	35 650	IIR	—	—

[a] Ref. 22. [b] Ref. 19.

tyramine[30] and synephrine,[31] in which the number of conformers can be completely explained by considering the OH rotamer of corresponding analogs, phenylethylamine[30] and 2-methylamino-1-phenylethanol (MAPE),[31] which have no phenolic OH. If the same rule is applied to Tyr, not 8 but 12 conformers should be observed.

In this work, we remeasured REMPI and HB spectra of Tyr by laser desorption supersonic jet technique and successfully observed the origin bands of 12 conformers. Furthermore, IR dip spectroscopy was applied to reassign their structures. Based on these new results, we will discuss a conformational evolution of Phe → Tyr → dopa which is an analog of Tyr and has one more phenolic OH at the *meta*-position with respect to the amino-acid chain.

II. Experimental

REMPI and HB spectroscopy were employed to measure the electronic spectra and to distinguish the electronic transition of each conformer. To measure the IR spectra, we applied IR dip spectroscopy. The principles of these spectroscopies are described in our previous reports[32–35] as well as the setup for the laser desorption. Briefly, Tyr (Aldrich) without further purification was mixed with carbon black powder (1 : 1 by weight) and applied to the lateral face of a graphite disk (diameter: 120 mm, thickness: 4 mm). The disk was placed

just under a pulsed nozzle (Even-Lavie pulsed valve),[36] and turned at a speed of one revolution per hour to provide fresh material constantly. The sample was desorbed by 1064 nm radiation of a Nd^{3+}:YAG laser (New Wave: Minilase II), and the sample vapor was picked up by a supersonic expansion of Ar whose stagnation pressure was 40 bar, and was efficiently cooled down by a collisional cooling. The supersonic jet was trimmed to a molecular beam by a skimmer with 2 mm diameter, and crossed with a tunable UV laser in the extraction region of a linear time-of-flight mass spectrometer to measure the REMPI spectra. The UV laser for the REMPI spectroscopy and a probe laser of HB spectroscopy was generated by a frequency-doubled dye laser (Lumonics: HD-500, Inrad: AUTOTRACKER III with BBO crystal) pumped by a third harmonic of a Nd^{3+}:YAG laser (LOTIS-TII: LS-2137). A second tunable UV laser for a burn laser of HB spectroscopy was generated by a frequency-doubled dye laser (Sirah: Cobra-Stretch, Inrad: AUTOTRACKER III with BBO crystal) pumped by the third harmonic of a Nd^{3+}:YAG laser (Continuum: Surelite-II). A tunable IR laser for the IR dip spectroscopy was generated by difference-frequency mixing, using the output of a dye laser (Fine Adjustment: Pulsare-S Pro) pumped by a 50% output of a second harmonic of a Nd^{3+}:YAG laser (Spectra Physics: PRO-230) and a 10% output of the second harmonic in a $LiNbO_3$ crystal. The desorption laser and the first UV laser were operated at 20 Hz, while the second UV laser and the IR laser were at 10 Hz to obtain a UV only signal and two color signals (UV + UV or UV + IR) alternately. By dividing the latter by the former, the fluctuations in the condition of the laser desorption source can be canceled.[37] The produced cation was detected by a home-made dynode converter detector[38] through a time-of-flight mass spectrometer. The signal was amplified by a preamplifier (NF: BX-31A) and was measured by a PCI fast digitizer board (Acqiris: U1082A-SSR). The Tyr mass peak was picked up from the acquired wave, and its area was averaged by tandem exponential moving average method[39] and recorded as a function of the wavelength of a scanning laser.

We carried out density functional theory (DFT) calculations to obtain the probable structures and the theoretical IR spectra of Tyr. Initial structures for the optimization were obtained by CONFLEX,[40,41] which is a conformational analysis system using force field calculations. To optimize structures and calculate their relative stabilization energy, we tested several functionals, B3LYP, CAM-B3LYP, M062X and wB97XD with a basis function of cc-pVDZ. The theoretical IR spectra were calculated at the CAM-B3LYP/cc-pVTZ level with a linear scaling factor of 0.94748 which was determined by comparing the calculated frequency of OH stretching of phenol with the observed one.[42] All quantum chemical calculations were carried out by utilizing GAUSSIAN 09.[43]

III. Results and discussions

III-1. REMPI and HB spectra

Fig. 2a shows a REMPI spectrum of Tyr in a supersonic molecular beam. The spectrum presents well-resolved sharp vibronic

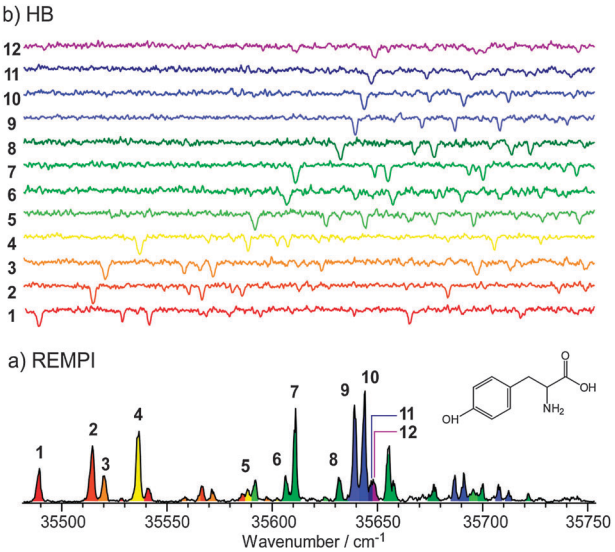

Fig. 2 REMPI spectrum (a) and HB spectra (b) of tyrosine. Each HB spectrum was measured by monitoring each 1–12 band observed in the REMPI spectrum.

structures, thus the Tyr molecules are cooled down sufficiently by the high pressure jet expansion. The observed spectrum is essentially the same as the REMPI spectrum reported by de Vries and co-workers,[22] and the intensity distribution between the vibronic bands is different from the LIF spectrum reported by Levy and co-workers[3] and Ebata and co-workers.[19] This is explained by the fact that the lifetime, which reflects a non-radiative process, varies from 3.5 to 7.9 ns depending on the conformer.[19]

The complicated structures in the electronic transition of Tyr were explained by coexistence of conformers. Seven independent transitions were identified and were assigned to eight isomers by the de Vries group with HB spectroscopy. The origins of the assigned isomers are indicated in the Figure by numbers 1, 2, 3, 4, 7, 9 and 10, which correspond to the A–G isomers in the notation of de Vries' report, respectively.[22] Here, the band indicated by number 7 is interpreted to the overlapping band of two isomers. The vibronic bands other than these seven bands are assigned to the vibronic transitions of one of the isomers. Ebata and coworkers also assigned the same seven bands to the origin of eight isomers although the correspondence between the band and the conformation is different from that of de Vries group's. The assignments look reasonable, however the number of isomers are less than 12, which is expected from the 6 isomers in phenylalanine as was described in Introduction.

To solve the inconsistency, we measured the HB spectra by labeling almost all the bands except for some apparent vibronic bands of known isomers. The observed HB spectra are shown in Fig. 2b. The labeled band is indicated beside the spectra. The HB spectra obtained by labeling the bands 1, 2, 3, 4, 7, 9 and 10 are the same as those reported in previous works.[19,22] The most important difference from the previously reported HB spectra is that the five HB spectra obtained by probing bands indicated 5, 6, 8, 11 and 12, which have been assigned to the vibronic

bands, present independent vibronic structures. This strongly indicates that the bands indicated 5, 6, 8, 11 and 12 belong to new isomers. If so, the number of isomers in Tyr is 12, and matches the expected number 12, from the 6 conformers of phenylalanine.

Tyr is a *p*-hydroxylphenylalanine, and thus double the number of conformers in phenylalanine is expected from the *cis* and *trans* orientation of the OH group. It is known that *cis*- and *trans*-rotational isomers show almost the same electronic spectra. To compare the vibronic structures of the spectra, all the HB spectra are aligned to the relative wavenumbers from each origin band (Fig. 3). Similarly to the previous reports, it was found that these can be classified into six pairs of spectra on the basis of the similarity of the vibronic structures. The pairs of (1, 3), (2, 4), and (9, 10) have already been reported,[19,22] and are assigned to the *cis* and *trans* pairs of rotamers. Three pairs of (5, 6), (7, 8) and (11, 12) are newly found in this work. The classification of six pairs means that there are six conformations of the amino-acid chain, which corresponds to the number of conformers of phenylalanine in the gas phase. Thus we have concluded that the Tyr molecule has 12 conformers, rather than 8 conformers.

In the previous reports, the pair of *cis* and *trans* rotamers are picked up from their similar intensities in the REMPI spectrum. In actuality, the pairs of (1, 3), (2, 4) and (9, 10) show comparable transition intensities in the spectrum. The newly assigned pairs of (5, 6) and (11, 12) show the almost the same intensities between the *cis* and *trans* rotamers. In contrast, the pair of (7, 8) shows significantly unequal intensities: the band of number 8 is about 1/3 of the number 7 band. Such unequal intensities in the *cis* and *trans* rotamers will be discussed later. The observed 0–0 transition energy of each conformer and its assignment are listed in Table 1 together with the assignments of the previous works.

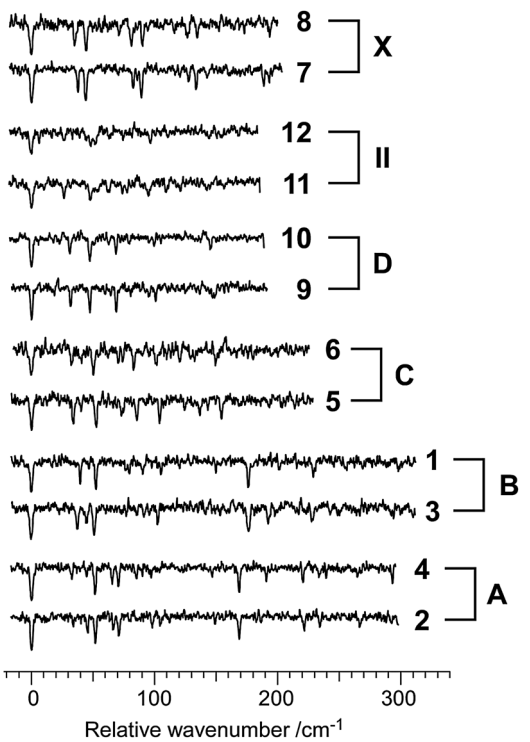

Fig. 3 HB spectra represented by relative wavelength with respect to each 0–0 transition and classified into similar pairs. The represented conformational assignments are results of further analyses in this work.

III-2. IR dip spectra

By fixing the wavelength of the UV laser to band 1–12, we measured IR dip spectra of twelve conformers (Fig. 4). Numbers beside the spectra show the band to which the UV laser was fixed. IR dip spectra obtained by probing bands 1, 2, 3, 4, 7, 9 and 10 have already been reported.[19,22] The observed spectra reproduce well the previous reports. The spectra measured by probing band 5, 6, 8, 11 and 12 are newly observed ones. These spectra show different vibrational structures from those in the previous reports. For example, the characteristic vibrational band of conformers 1 and 3 is a broad band at around 3290 cm^{-1}. This vibrational band cannot be seen in any of the newly observed spectra. The characteristic band at 3340 cm^{-1} in the conformers 2 and 4 also cannot be seen in the new spectra. The vibrational structure in the region from 2900 cm^{-1} to 3050 cm^{-1} of the conformers 9 and 10 is different from those in the new spectra. The spectrum obtained by exciting the band 8 is similar to that of the conformer 7, however, a broad vibrational band at about 3250 cm^{-1} is shifted to higher frequency. The spectral difference confirms that the bands 5, 6, 8, 11 and 12 are newly observed conformers.

The electronic spectra can be classified into 6 pairs according to the similarity of the spectral features, which arise from the 2 possible orientations of the phenolic OH. Such a classification can also be applied to the vibrational spectra. In Fig. 4, the spectra have been aligned according to the classification of the HB spectra. One can easily find spectral similarities within each pair, *i.e.* (2, 4), (1, 3), and so on (see the Figure). It also supports the analysis of the conformers based on *cis* and *trans* rotamers with the same amino-acid chain conformation.

In all the spectra, clusters of bands at 2900–3000 cm^{-1} and 3000–3100 cm^{-1}, a sharp band around 3420 cm^{-1} and a sharp and intense band at 3660 cm^{-1} are observed commonly. These bands are assigned to CH stretching of methylene, those of the benzene ring, hydrogen bonded NH_2 anti-symmetric stretching and free OH stretching of phenolic OH, respectively. A sharp and intense band at 3580 cm^{-1} (3565 cm^{-1} for 5 and 6) is observed in the spectra of conformers 2, 4, 5, 6 and 9–12 is assigned to free OH stretching of COOH. In the spectra of conformers 1, 3, 7 and 8, a broad intense band is observed around 3200–3300 cm^{-1}, which is assigned to hydrogen bonded OH stretching of COOH. This red-shifted and broad OH stretching of COOH is a signature of an OH → N type hydrogen bond, in which the OH of the carboxy group donates hydrogen to the nitrogen atom of the amino group.[19,22] Only in the spectra 2, 4, 7 and 8 is a weak band observed at ~3340 cm^{-1}, which is assigned to hydrogen bonded NH_2 symmetric stretch. The observed vibrational frequencies, except CH stretches, are listed in Table 2.

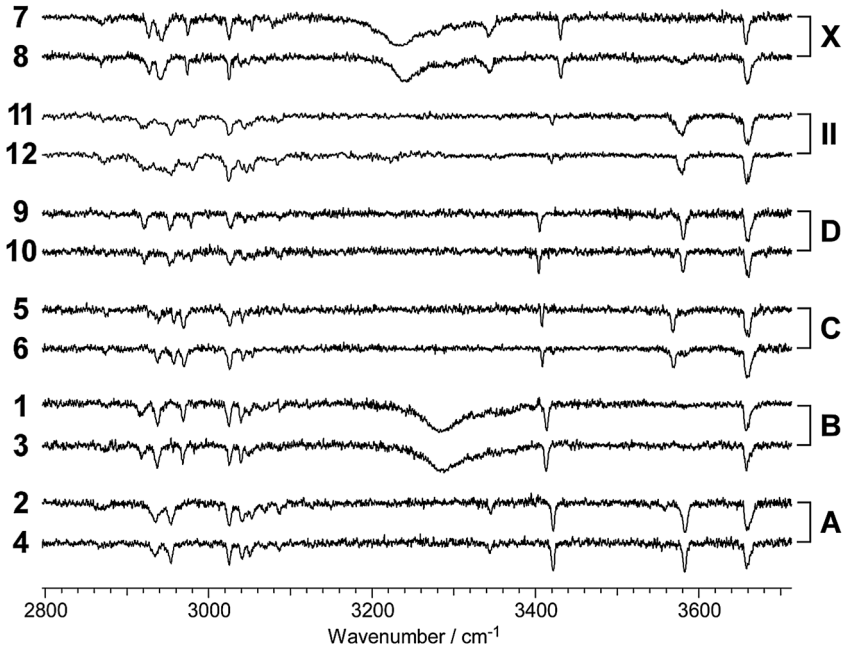

Fig. 4 IR dip spectra of each 12 conformers. The order is rearranged according to their similarities. The represented conformational assignments are results of further analyses in this work.

Table 2 Observed and calculated (in parentheses, CAM-B3LYP/cc-pVTZ with a linear scaling factor 0.94748) vibrational frequencies (cm^{-1})

Conformer	*sym*-NH_2	*anti*-NH_2	Carboxy OH	Phenolic OH	Conformational assignment
1	—	3411	3278[a]	3660	BS
	(3356)	(3422)	(3330)	(3657)	
2	3342	3419	3580	3660	AS
	(3351)	(3435)	(3582)	(3657)	
3	—	3411	3278[a]	3660	BR
	(3356)	(3422)	(3330)	(3657)	
4	3341	3419	3580	3660	AR
	(3351)	(3434)	(3582)	(3658)	
5	—	3405	3565	3660	CS
	(3337)	(3416)	(3570)	(3657)	
6	—	3405	3565	3660	CR
	(3336)	(3415)	(3570)	(3659)	
7	3338	3427	3229[a]	3660	XR
	(3345)	(3434)	(3311)	(3657)	
8	3340	3428	3236[a]	3660	XS
	(3345)	(3434)	(3315)	(3657)	
9	—	3401	3578	3660	DR
	(3345)	(3412)	(3582)	(3658)	
10	—	3401	3578	3660	DS
	(3345)	(3411)	(3582)	(3658)	
11	—	3416	3576	3660	IIS
	(3354)	(3427)	(3580)	(3658)	
12	—	3416	3576	3660	IIR
	(3354)	(3428)	(3581)	(3658)	
—	(3367)	(3451)	(3587)	(3659)	ES
—	(3366)	(3451)	(3587)	(3658)	ER
—	(3354)	(3432)	(3336)	(3658)	IS
—	(3353)	(3432)	(3336)	(3658)	IR
—	(3342)	(3412)	(3579)	(3659)	IIIS
—	(3341)	(3411)	(3579)	(3658)	IIIR

[a] Broad band.

III-3. Computational prediction of stable conformers

To investigate the structures of the conformers, we calculated the stabilization energies, optimized geometries and theoretical IR spectra for various conformers of Tyr. Quantum chemical calculation has already been reported by Zhang *et al.*,[9] however, they used the DFT method with a B3LYP functional and the MP2 method. The former underestimates and the latter overestimates dispersion interactions. Nowadays, it is known that DFT methods with dispersion corrections are suitable for calculation of flexible molecules. Recently, Baek *et al.* reported the DFT calculations of Tyr at the M05-2X/6-311+G* level, which involves dispersion correction, and they found 18 stable conformers.[23] However, the most suitable functional depends on the system, thus it is important to compare the calculated results by not only M05-2X but also other functionals. Here, we carried out DFT calculations with several dispersion-corrected functionals, CAM-B3LYP, M062X and wB97XD, to predict stable conformers of Tyr.

Prior to the DFT calculations, the CONFLEX program was employed to search conformations to generate initial structures for the DFT. From the force field analyses, 61 structures were obtained. These structures were used as initial structures of optimization at B3LYP/cc-pVDZ, and 57 different stable conformers were obtained. These optimized structures contain non-hydrogen-bonding structures, which are apparently unstable. From the output, we picked up 44 conformers which form hydrogen bonds in the amino-acid chain. By using these structures as initial structures, we calculated the optimized structure at CAM-B3LYP, M062X and wB97XD with the basis set of cc-pVDZ.

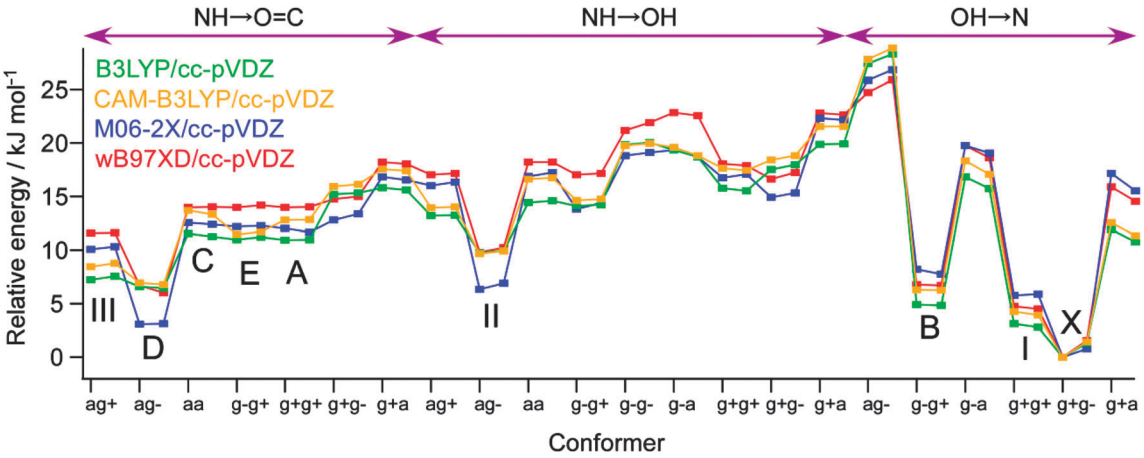

Fig. 5 Relative stabilization energies obtained by several DFT methods with zero point energy correction. Notations of conformations are mentioned in the manuscript. Each pair that has the same conformational notation is in related of the phenolic OH rotamers, which are represented in order of R and S.

To discriminate each structure of these 44 conformers, we use the same systematic notations as used in dopa.[44] Briefly, the hydrogen bonding patterns of the amino-acid chain are classified into three types:(1) OH → N (OHN), in which the OH of the carboxy group donates hydrogen to the nitrogen atom of amino group; (2) NH → O═C (NHOC), in which one or two hydrogen atom of the amino group donates to the carbonyl oxygen atom; and (3) NH → OH (NHOH), in which one or two hydrogen atom of the amino group donates to the oxygen atom of carboxy group. In addition, the conformations of the amino-acid chain are classified by dihedral angle of N–C_α and C_α–C_β. In each case, notations of a (anti), g+ (gauche +) and g− are used. Finally the orientations of the phenolic OH should be distinguished. Generally, to distinguish the phenolic OH orientation, notations of *cis* and *trans* are used. Such notations are better for intuitive understanding, however, ambiguity in the conformational definitions arises in some conformations. Therefore, we adopt notations of R and S as in our previous paper,[44] which mean the absolute configuration around C_β when viewed from the direction in which the phenolic OH is pointing.

Fig. 5 shows plots of relative stabilization energies for the 44 conformers obtained by several DFT methods. The types of hydrogen bonding are indicated in the top of the Figure. The lower horizontal axis shows the conformation of the amino-acid chain. The pair of rotamers R and S for phenolic OH are plotted side by side. The values of calculated energies are listed in the ESI.† For convenience, the conformers corresponding to the observed conformers in phenylalanine are indicated by the letters A–E and X in the Figure. It is found that OHNg+g−R and OHNg+g−S, which have the same amino-acid conformation as the conformer X in phenylalanine, are the most and secondary stable conformers regardless of the calculation methods. However the next stable conformer indicated by the letter I is not related to the conformations A–E. As can be seen in the Figure, three amino-acid conformations (6 conformers because of R and S rotamers) are more stable than the conformation C, which is the least stable one in A–E. The three conformations are indicated by the letters I–III. The order of the stabilization energies of the conformations A–E, X and I–III depend on the method of calculation, however, these 9 conformations in the amino-acid chain (18 conformers) cover the most stable 18 conformations in all the calculations.

The 18 calculated structures originated from the R and S rotamers of A–E, X, I, II and III amino-acid chain conformations at the CAM-B3LYP/cc-pVDZ level are shown in Fig. 6. All the structures of 44 conformers are given in the ESI.† These 18 conformers are almost the same as those reported by Baek *et al.* (M05-2X/6-311+G*)[23] except for conformers C, which show a significant discrepancy with a dihedral angle of O═C–C^α–N. At the CAM-B3LYP/cc-pVDZ level, the dihedral angle of O═C–C^α–N is calculated to be 93.0°, while 48.0° was reported by using the M05-2X/6-311+G* level. The calculations at the M06-2X/cc-pVDZ and wB97XD/cc-pVDZ levels give 41.9° and 45.8°, which are similar to the result at the M05-2X/6-311+G* level.

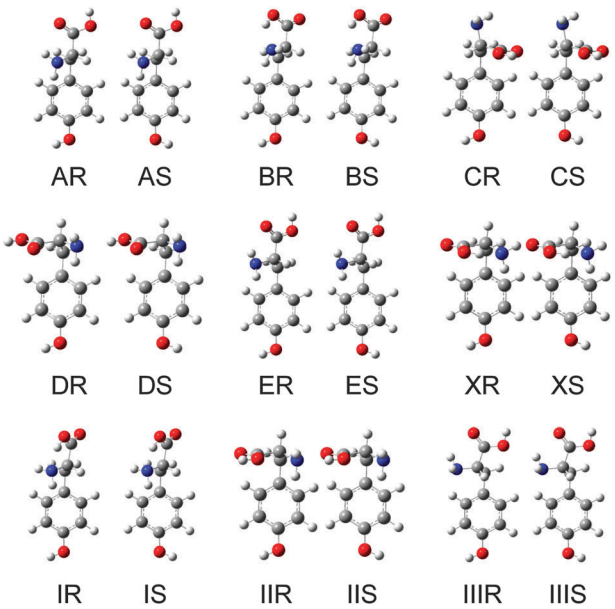

Fig. 6 18 Stable conformers of tyrosine predicted by CAM-B3LYP/cc-pVDZ.

This means that the structure of conformers C is strongly depends on dispersion interaction, because subtle difference of dispersion correction between the functionals causes a large difference in the geometry.

III-4. Structural assignments of each conformer

To determine the structures of the observed conformers, we compared the observed conformer-selective IR spectra with the theoretical ones for the optimized structures shown in Fig. 6. The IR spectra of Phe, whose assignments are established,[5,8] are also referenced to assign the conformation of Tyr. Here, M06-2X and wB97XD functionals predict that the frequency of OH stretching of COOH, which forms an OHN hydrogen bond, is higher than the symmetric stretching of NH_2. This causes apparent conflicts with the experimental results. On the other hand, the CAM-B3LYP functional predicts the frequencies of the hydrogen bonded OH stretching at an adequate position. Therefore we adopted the results of CAM-B3LYP functional for the assignment of IR spectra. We used the basis set of cc-pVTZ for the vibrational analyses. The basis set cc-pVDZ is already good enough to reproduce NH bonds but this basis set improves the better reproduction of the hydrogen bonded OH stretching. It should be noted that the difference of vibrational frequencies among conformers are clear in the observation, however the theoretical reproduction at the absolute frequencies is still challenging because of anharmonicity. Further improvement in assignments may be possible by the high level calculations that take into account anharmonicity. Here we would like to discuss the best possible assignments from the harmonic theoretical calculations and experimental consistencies including the conformational assignments in Phe.

From the spectral features, pairs of conformers, (1, 3) and (7, 8), obviously form the OHN-type hydrogen bond. Thus, we compared their observed IR spectra with theoretical ones of B, X and I (Fig. 7). There are two clearly different points between the conformers (1, 3) and (7, 8). One is that the frequency of the carboxy OH stretching of conformers (7, 8) is red-shifted by $\sim$50 cm^{-1} from that of (1, 3), and another is that the symmetric stretching of NH_2 is observed in conformers (7, 8), whose intensity is the almost comparable with anti-symmetric stretching, while it is not observed in (1, 3). In the theoretical spectra, frequencies of the carboxy OH stretchings and intensity patterns of the NH_2 stretchings are different among conformers B, X and I. In the conformers X, the frequencies of the carboxy OH stretching are predicted at the lowest energy among the 3 conformers. The intensity of the symmetric stretching of NH_2 is comparable to that of anti-symmetric stretching. These spectral features correspond to those of conformers (7, 8). In addition, the frequencies of the NH_2 stretchings of conformers X reproduce well those of conformers (7, 8). Therefore, conformers (7, 8) are assigned to conformers X. Furthermore, in the observed spectra of conformers (7, 8), not much but a clear difference (7 cm^{-1}) was found in the frequency of carboxy OH stretching between them. Such frequency difference is reproduced only in the rotamer pair of the conformers X at several calculation levels (see Table S1, ESI†). Thus this result supports the above

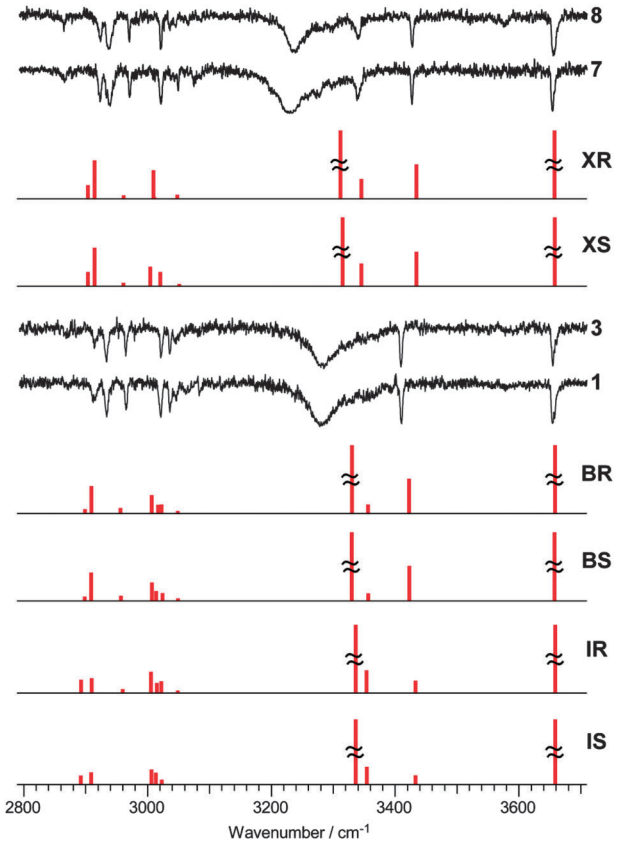

Fig. 7 Comparison of the observed IR dip spectra of conformers (1, 3) and (7, 8) with theoretical IR spectra calculated by CAM-B3LYP/cc-pVTZ with a linear scaling factor 0.94748.

assignment and makes it possible to describe the assignment of phenolic OH rotamers, *i.e.*, the conformers 7 and 8 can be assigned to XR and XS, respectively. On the other hand, by comparing the intensity patterns of NH_2 stretchings between conformers B and I, it was found that the intensity of the anti-symmetric stretching is much larger than that of symmetric stretching in conformers B, while symmetric stretching is slightly stronger than anti-symmetric stretching in the conformers I. The former corresponds to the observed spectral feature of conformers (1, 3). In addition, the frequency of the anti-symmetric stretching shows a good agreement between conformers B and (1, 3). Therefore, conformers (1, 3) are assigned to conformers B.

By comparing the calculated frequencies of conformers B and X with the observed ones (see Table 2), it was found that the NH_2 stretchings are reproduced well (5–10 cm^{-1} higher than observed) by the used calculation level, while the hydrogen bonded carboxy OH stretchings are predicted at 60–70 cm^{-1} higher than the observed ones. Such a discrepancy is derived from the large anharmonicity of strongly hydrogen bonded OH stretching. To improve the calculated frequencies of such vibrational modes, anharmonic vibrational analyses should be necessary.[45–50]

The rest of the conformers, *i.e.* (2, 4), (5, 6), (9, 10) and (11, 12), were compared to the theoretical IR spectra of conformations A, C, D, E, II and III, which have an NHOC or NHOH-type hydrogen

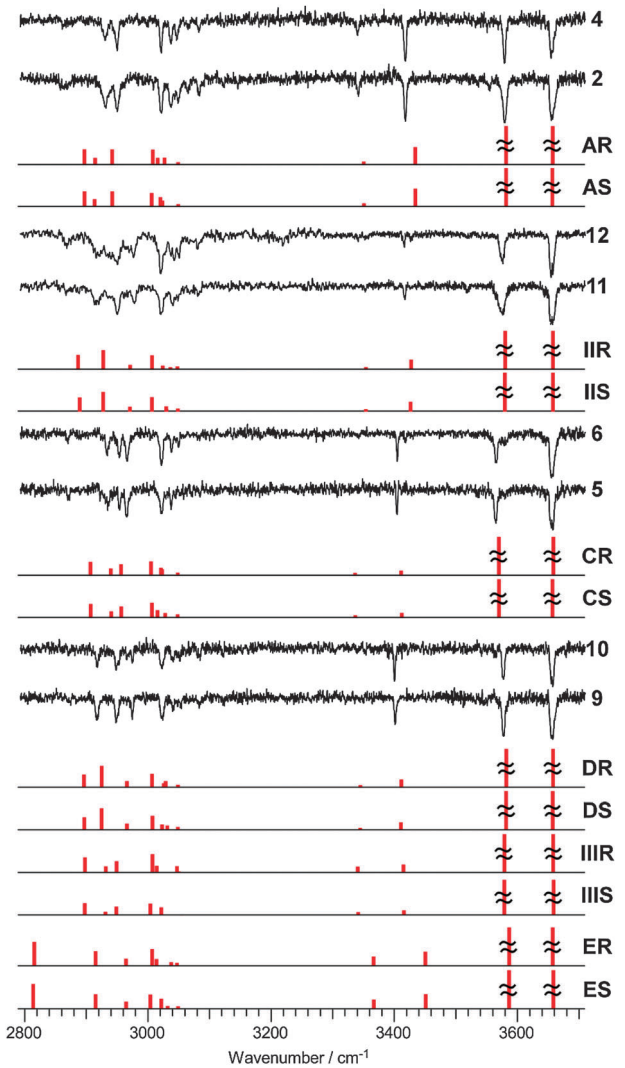

Fig. 8 Comparison of the observed IR dip spectra of conformers (2, 4), (5, 6), (9, 10) and (11, 12) with theoretical IR spectra calculated by CAM-B3LYP/cc-pVTZ with a linear scaling factor 0.94748.

bond (Fig. 8). Here, we will assign the conformation of the amino-acid chain. In the observed spectra, the most remarkable difference was found in anti-symmetric stretching of NH_2 (*anti*-NH_2) at ~3400 cm^{-1}. The vibrational frequencies are 3419, 3416, 3405 and 3401 cm^{-1} for the conformer pairs (2, 4), (11, 12), (5, 6) and (9, 10), respectively. Such a shift of *anti*-NH_2 according to the conformers has been reported in the IR spectra of Phe.[5,7] The observed frequencies for Phe are plotted by us in Fig. 9 for conformations A, C, D and E. The theoretical calculations for Tyr also show the frequency-shift of *anti*-NH_2 for the conformation of the amino-acid chain, as shown in Fig. 9. Circles show the calculated frequencies with a scaling factor of 0.94748. The calculated frequencies of the A–E conformers of Tyr are uniformly higher than the observed ones of Phe, nonetheless their energetic tendencies are well-reproduced by the calculations. To estimate the frequencies of conformers II and III, which are not observed in Phe, the theoretical frequencies for Tyr were scaled linearly again.

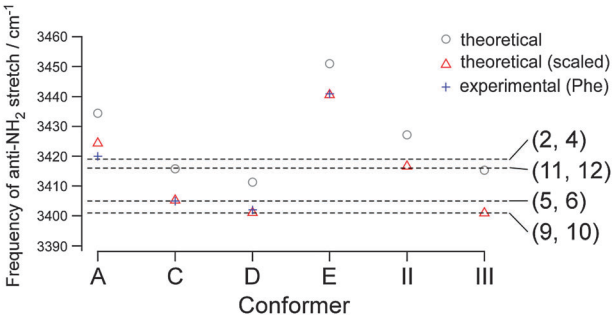

Fig. 9 Vibrational frequencies of anti-symmetric stretching of NH_2 of each conformer. Dashed lines indicate observed frequencies by monitoring each pair of phenolic OH rotamers.

The scaled frequencies are represented by triangles. The second scaling factor (0.9970) was determined by the least squares method. Since these doubly scaled frequencies (triangles) of A–E conformers of Tyr reproduce well those of Phe, those of conformers II and III should be quantitatively reasonable. Here, let us compare the observed frequencies of conformers (2, 4), (5, 6), (9, 10) and (11, 12), which are shown by dashed horizontal lines in the Figure, with the doubly scaled calculated frequencies. The observed conformers can be classified in two groups according to the observed frequencies of *anti*-NH_2. One is a group whose frequency is observed at higher than 3410 cm^{-1} (conformers (2, 4) and (11, 12)) and another is lower (conformers (5, 6) and (9, 10)). Also the doubly scaled calculated frequencies can be classified in the same manner. Based on this tendency, conformers (2, 4) and (11, 12) are assigned to A, E or II conformers. Since the calculated frequency of E is remarkably higher than the others, so it can be ruled out from the candidates. The calculated frequency of conformer A is slightly higher than that of conformer II, thus, we tentatively assign conformers (2, 4) and (11, 12) to the A and II conformers, respectively, according to the order of frequencies. The adequacy of this assignment will be discussed later by comparing with the frequencies of Phe. Similarly, conformers (5, 6) can be tentatively assigned to C, and (9, 10) to D or III.

A different point between the (2, 4) and (11, 12) pairs is the intensity of the *anti*-NH_2. The former gives a more intense band than the latter. Also in the calculated spectra of conformer A and II, a similar difference of transition intensity is predicted, which supports the above assignment; *i.e.* of the (2, 4) and (11, 12) pairs to conformers A and II, respectively. However, the difference of the 0–0 transition intensity of each pair ((2, 4) is stronger than (11, 12)) is inconsistent with the calculated relative stability of conformers A and II. Such inconsistencies are also found in Phe, which is related to the systematic formation of conformers.[51]

In another group, (5, 6) and (9, 10), we can find a difference also in the frequency of carboxy OH stretching. The frequency is 3565 cm^{-1} for the conformers (5, 6), which is the lowest among the NHOC or NHOH-type hydrogen bond family, while it is 3578 cm^{-1} for (9, 10). This shift is reproduced by the calculations, actually, the conformer C shows the lowest frequency among not only C, D

and III but also the NHOC or NHOH-type hydrogen bond family, which supports the assignment of the conformers (5, 6) to C. On the other hand, it is difficult to determine which the (9, 10) pair is assigned to conformer D or III only by the IR spectrum. The calculated IR spectra of conformer D and III are almost the same, except for the CH stretching region. Generally the CH stretching modes easily cause anharmonic coupling and need high-accuracy anharmonic vibrational analyses to be predicted theoretically. Here we took notice of the 0–0 transition intensity. The bands 9 and 10 are the strongest and the second strongest transitions in the REMPI spectrum. This suggests that these conformers are significantly stable. In all the calculations performed in this work, the conformer D is more stable by 3–8 kJ mol^{-1} (by dispersion correction methods) than conformer III (see Fig. 5). In addition, the conformer D of Phe gives the most intense 0–0 band in REMPI spectrum.[5,7] Thus it is reasonable that the (9, 10) pair is assigned to the conformer D.

In summary, we have tentatively assigned the conformation of the amino-acid chain in the (2, 4), (5, 6), (9, 10) and (11, 12) pairs to the conformations A, C, D and II, respectively.

Here, the observed frequencies of the NH and OH stretching of the amino-acid chain are compared with those of Phe (see Table 3). As shown in the Table, all frequencies of Tyr except conformers IIR/S and XR show good agreement with those of the corresponding conformer of Phe. Since the phenolic OH of Tyr is too far from the amino acid chain to interact strongly, this result indicates that our assignments of the amino-acid conformations of Tyr are appropriate. In addition, it is also shown that conformers E are not observed in Tyr and the conformer XR has an obvious interaction between the phenolic OH and the amino-acid chain which will be discussed later.

Table 3 Comparison of the observed vibrational frequencies (cm^{-1}) of phenylalanine (ref. 5, 8) and tyrosine

Conformational assignment	*sym*-NH_2	*anti*-NH_2	Carboxy OH
Phe(A)	3342	3420	3581
Tyr(AR)	3341	3419	3580
Tyr(AS)	3342	3419	3580
Phe(B)	3351	3411	3280
Tyr(BR)	—	3411	3278
Tyr(BS)	—	3411	3278
Phe(C)	3370	3405	3567
Tyr(CR)	—	3405	3565
Tyr(CS)	—	3405	3565
Phe(D)	3342	3402	3579
Tyr(DR)	—	3401	3578
Tyr(DS)	—	3401	3578
Phe(E)	3363	3441	3587
Tyr(IIR)	—	3416	3576
Tyr(IIS)	—	3416	3576
Phe(X)	3341	3428	3235
Tyr(XR)	3338	3427	3229
Tyr(XS)	3340	3428	3236

So far, the conformation of the amino-acid chain has been assigned for all the conformers of Tyr, however the orientation of phenolic OH has not been determined yet, except for the conformers 7 and 8. It is because the amino-acid chain and OH locate at the *para* position in the benzene ring and the OH stretching frequency is mostly unperturbed by its orientation. Instead of the vibrational frequencies, we focused on the electronic transition intensities of rotamer pairs in the REMPI spectrum. The transition intensity is proportional to the population in S_0, which reflect the relative stabilization energy. For the (2, 4) bands which are assigned to the conformation A for their amino acid chain, the band 4 is slightly stronger than the band 2. However, stabilization energy differences between the rotamers predicted by the theoretical calculations are not significant, for instance, AR is more stable by 0.05 kJ mol^{-1} than AS. Such a tiny difference cannot be adopted as a criterion to assign the rotamers. In our previous paper,[31,44] we reported that the orientation of the phenolic OH can be rationalized by a dipole–dipole interaction between the OH group and the amino acid chain. The dipole–dipole interaction is rather insensitive to the calculation level[44] and thus the energy difference in the dipole–dipole interaction can be a good criterion for the tentative assignments of the rotamers. The dipole–dipole interaction energies between the phenolic OH group and the amino-acid chain was calculated from the optimized geometries discussed in the previous section. Based on them and the relative intensities in the REMPI spectrum, the rotamers are assigned as shown in Table 1. The details of the dipole–dipole interactions are discussed in the next section particularly for XR and XS.

The previous assignments by the de Vries group and the Ebata group are compared in the Table. Our assignments are rather similar to those by the de Vries group, although they did not assign the conformations C and II, and XS. Particularly, the lack of the assignment for XS is noteworthy. The previous groups assumed that the OH rotamers should have comparable transition intensities in the REMPI spectrum, and tried to find the counterpart of the band 7. As can be seen in the REMPI spectrum (Fig. 2), the bands 9 and 10 have comparable intensities to the band 7, however, the conformer selective IR spectra prove that the band 9 and 10 have the same amino-acid conformation and thus cannot be assigned to the partner of the band 7. That is why the previous reports assigned that the band 7 did not correspond to a single conformer but two conformers that have the same amino-acid conformation X. In our assignments, XS is assigned to the band 8, of which the intensity is 1/3 of the band 7. Such intensity deviation in the rotamer pairs caused confusion in the previous assignments. The intensity deviation between XR and XS will be fully discussed in the next section.

III-5. Characteristic behaviors of conformers XR and XS

The conformer XR shows two characteristic behaviors: (1) specific stability, which leads a large stability difference between two rotamers, XR and XS, in the intensity of the 0–0 transition; and (2) a red-shift of the hydrogen bonded OH of COOH. These phenomena clearly demonstrate that interactions

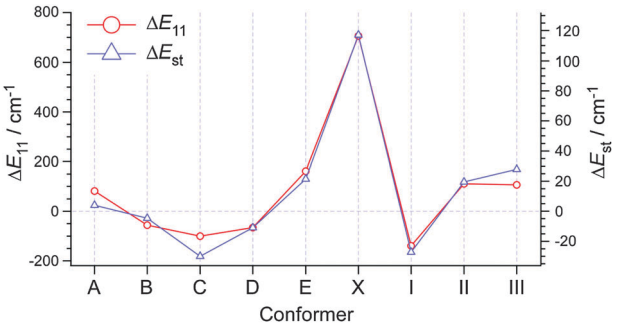

Fig. 10 Dipole–dipole interaction energy difference ($\Delta E_{11} = E_{11}(S) - E_{11}(R)$) and stabilization energy difference ($\Delta E_{st} = E_{st}(S) - E_{st}(R)$) between R and S rotamers of each conformer. Stabilization energies ($E_{st}(S)$, $E_{st}(R)$) were calculated by CAM-B3LYP/cc-pVDZ with zero point energy correction.

between the phenolic OH and the amino-acid chain exist. The distance between them is too great to interact directly as intramolecular hydrogen bonds. As mentioned in our previous paper, such interaction can be explained by dipole–dipole interaction.[31,44] Actually, as shown in Fig. 10, the dipole–dipole interaction the energy difference is the largest in the X conformers, which means that the stabilization by the dipole–dipole interaction is the largest in the conformer XR. This can be explained by direction of the partial dipole moment of the amino-acid chain. Fig. 11 shows definitions of the parameters to formulate the dipole–dipole interaction energy (J),

$$V_{11} = -\frac{\mu_1\mu_2}{4\pi\varepsilon_0 r^3}(2\cos\theta_1\cos\theta_2 - \sin\theta_1\sin\theta_2\cos\phi). \qquad (1)$$

Each angle can adopt a value from 0 to π independently. Thus, in the most stable orientation, the dihedral angle ϕ must be π, because $\sin\theta_1\sin\theta_2$ is always positive. In such case, the inside of the parentheses can be written as $\cos\theta_1\cos\theta_2 + \cos(\theta_1 - \theta_2)$, here θ_1 and θ_2 are independent, so both of them must be equal to 0 for the most stable orientation. Therefore, the dipole aligned formation, in which one dipole points to the end of another dipole, gives the most stable dipole–dipole interaction energy, as can be seen in the α-helix of polypeptides. However, such orientation cannot be realized in the Tyr case, because the phenolic OH cannot point to the amino-acid chain and thus θ_2 is roughly π/2. In such case, the inside of the

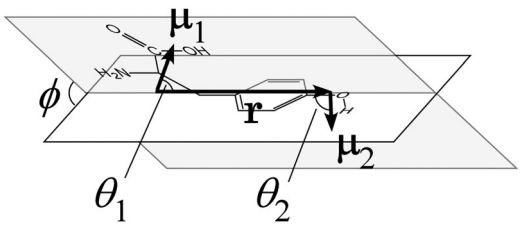

Fig. 11 Schematic diagram of the two partial dipole moments and their relative configuration. Electric dipole moments of the amino-acid chain and OH group are represented by μ_1 and μ_2, respectively. A vector from the charge center of the amino-acid chain to that of OH group is represented by **r**. θ_1 and θ_2 are angles between μ_1 and an axis along **r** and between μ_2 and the axis, respectively. ϕ is a dihedral angle between μ_1 and μ_2.

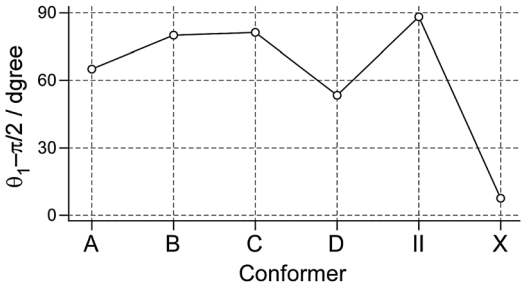

Fig. 12 Orientations of the partial dipole moment of the amino-acid chain in each conformer.

parentheses of eqn (1) is equal to $-\sin\theta_1\cos\phi$, which adopts a maximum value when $\theta_1 = \pi/2$ and $\phi = \pi$. Thus, the most stable geometry is achieved by an anti-parallel orientation of the two dipoles. We estimated the angle $\theta_1 - \pi/2$ (Fig. 12). At a glance, it is easily found that the angle is almost 0 only in the conformer XR. Thus, the specific stabilization due to the dipole–dipole interaction can be seen only in the conformer XR.

On the other hand, it is not straightforward to explain the enhancement of the hydrogen bond strength in the conformer XR, because the phenomenon itself is real but tiny. However, the same phenomenon is observed in dopa, in which the observed single conformer is specifically stabilized by the dipole–dipole interaction between the catecholic OHs and the amino-acid chain.[44] In dopa, the vibrational frequency of hydrogen-bonded OH stretch of COOH is observed at 3205 cm^{-1}, which is red-shifted by 30 cm^{-1} from that of Phe. One plausible interpretation to rationalize this phenomenon is that the formation of the strong hydrogen bond within the amino-acid chain is stabilized by the specifically strong dipole–dipole interaction.

III-6. Conformational evolution from phenylalanine to dopa *via* tyrosine

As mentioned in the Introduction, the conformations of Tyr should correlate with those of Phe, because the difference between them is whether phenolic OH exists at the *para*-position with respect to the amino-acid chain or not. In addition, by introducing one more phenolic OH to Tyr at the *meta*-position with respect to the amino-acid chain, Tyr evolves to dopa, so the structures of dopa should also correlate with Tyr. The number of conformers and their structures of dopa have already been reported, and it was found that only one conformer is observed in dopa.[44] This drastic reduction in the number of conformers is surprising and intriguing. To discuss the mechanism of the conformational reduction, tracing the conformational evolution from Phe to dopa might drop a hint. Thus we traced the conformational evolution of Phe → Tyr → dopa (Fig. 13).

The conformers A–D and X of Phe grow into AR, AS,..., *etc.* of Tyr, however, the conformer E does not appear in Tyr. Instead, conformer II, which is not observed in Phe, appears in Tyr. Also in Phe, the conformer II is more stable than A and E.[6] However, the conformer II is not observed in Phe.

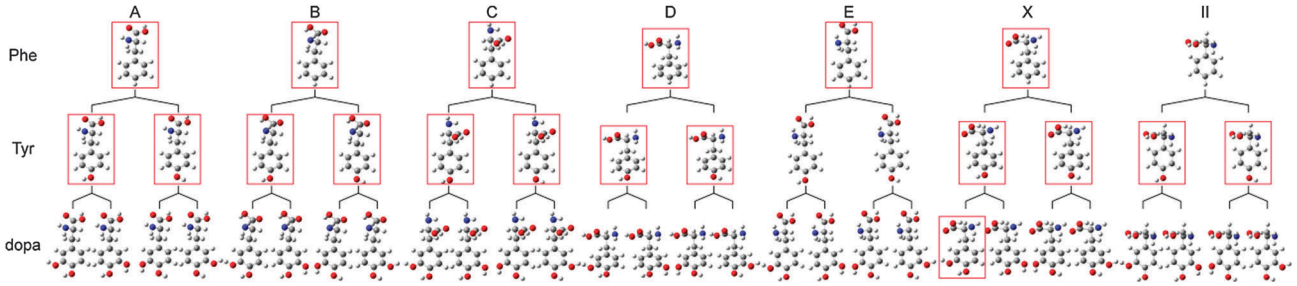

Fig. 13 Conformational evolution from phenylalanine to dopa *via* tyrosine. Conformers framed by rectangles are observed in a supersonic jet.

This nonequilibrium behavior was discussed by von Helden *et al.*[51] They interpreted that such conformers that are not observed, despite their higher stability than some of the observed ones, play the role of funnels for other observed conformers. Of course, the unobserved stable conformers are separated by certain barriers from other conformers; however, by generating a transient short lived collisional complex with a carrier gas molecule, they can have an internal energy lower than the dissociation energy of the complex which may lead to the conformational transformation to more stable conformers. In fact, von Helden *et al.* reported that the population of conformer E is enhanced by changing the carrier gas of Ar to Ne. This result suggests that the carrier gas of Ar, which has larger binding energy than Ne, has an ''annealing effect''. Recently, such an effect with solvent molecules was reported by Sohn *et al.*[52,53] They found that the distribution ratio of rotamers in *meta*-substituted phenols can be changed by seeding solvent molecules, H_2O, NH_3, CO_2,... *etc.* to the carrier gas, and the transformation from the metastable to the most stable rotamer takes place only when the binding energy between a solute (*m*-aminophenol) and a solvent molecule is larger than the barrier height of the transformation. The disappearance of the conformer E in Tyr may be interpreted by such an effect, however the appearance of the conformer II cannot be explained. Unfortunately, we do not have a clear view to interpret this phenomenon, but probably the change of the potential landscape due to the phenolic OH may affect the cooling process.

By comparing Tyr with dopa, it is found that conformer XR of Tyr grows into the most stable and exclusively observed conformer of dopa. This result clearly demonstrates that the phenolic and catecholic OHs stabilize a certain conformation of the amino-acid chain and this effect of the latter may be much larger than the former. However, it is also obvious that the conformational evolution from Tyr to dopa is unnatural, *i.e.*, all 24 conformers should be observed in dopa if the conformational evolution from phenylalanine to Tyr can be adopted for dopa. The stabilization energies of each conformer of dopa have already been reported in our previous paper.[44] The energy difference between the most stable and secondary stable conformer is about 250 cm^{-1} ($\sim$3 kJ mol^{-1}). This value, however, is not so large to give a biased conformational distribution (see Fig. 5). Therefore, the reason why only the most stable conformer is observed cannot be explained by the stabilization energy. Probably, the reduction of conformer in dopa will closely relate to topology of the potential landscape and the annealing effect within the jet-cooling process.

IV. Conclusions

By applying REMPI and HB spectroscopies to Tyr, the number of conformers in the supersonic jet was redetermined to 12. This number corresponds to 2 times that of phenylalanine, which is reasonable because, phenylalanine having 6 (A–E, X) conformers, means that the amino-acid chain adopts 6 conformations, and 2 different orientations of phenolic OH arise within each conformation of the amino-acid chain. However, the results of structural determination by the IR dip spectroscopy and quantum chemical calculations do not support such assignments. The conformers E are not observed in Tyr, instead other conformers (we represent II) are observed. This result may be explained by the differences of the jet-cooling process between Phe and Tyr, which however is not clear. Another curious result is the characteristic behavior of the most stable conformer XR. In other conformers, the stabilization energies of 2 rotamers according to the phenolic OH orientation are comparable, while the stabilization energy of the conformer XR is much larger than the conformer XS. This specific stabilization is explained by dipole–dipole interaction between the phenolic OH and the amino-acid chain. In addition, an anomalous red-shift is observed in the hydrogen bonding OH of the amino-acid chain only in the conformer XR. The cause of this phenomenon is not clear, but is probably due to the strong dipole–dipole interaction. The exclusively observed conformer in dopa is derived from the conformer XR; in fact the same phenomena are observed also in dopa. However, the reason why only one conformer is observed in dopa cannot be explained by the specific stability, because the energy difference between the most and secondary stable conformer is the almost same between Tyr and dopa. To clarify the mechanism of the conformational reduction observed in dopa, not only the potential landscape but also the annealing effect during jet-cooling process should be considered.

Acknowledgements

This study was supported in part by a Grant-in-Aid for Scientific Research KAKENHI in the priority area ''Molecular Science for

Supra Functional Systems'' from the Ministry of Education, Culture, Sports, Science and Technology (MEXT) Japan, and Industrial Technology Research Grant Program in 2006, and was performed under the Cooperative Research Program of ''Network Joint Research Center for Materials and Devices''.

References

1 J. P. Shermann, *Spectroscopy and Modeling of Biomolecular Building Blocks*, Elsevier Science, 2007.
2 S. J. Martinez, J. C. Alfano and D. H. Levy, *J. Mol. Spectrosc.*, 1991, **145**, 100–111.
3 S. J. Martinez, J. C. Alfano and D. H. Levy, *J. Mol. Spectrosc.*, 1992, **156**, 421–430.
4 S. J. Martinez, J. C. Alfano and D. H. Levy, *J. Mol. Spectrosc.*, 1993, **158**, 82–92.
5 L. C. Snoek, E. G. Robertson, R. T. Kroemer and J. P. Simons, *Chem. Phys. Lett.*, 2000, **321**, 49–56.
6 Y. H. Lee, J. W. Jung, B. Kim, P. Butz, L. C. Snoek, R. T. Kroemer and J. P. Simons, *J. Phys. Chem. A*, 2004, **108**, 69–73.
7 T. Ebata, T. Hashimoto, T. Ito, Y. Inokuchi, F. Altunsu, B. Brutschy and P. Tarakeshwar, *Phys. Chem. Chem. Phys.*, 2006, **8**, 4783–4791.
8 T. Hashimoto, Y. Takasu, Y. Yamada and T. Ebata, *Chem. Phys. Lett.*, 2006, **421**, 227–231.
9 W. H. Zhang, V. Carravetta, O. Plekan, V. Feyer, R. Richter, M. Coreno and K. C. Prince, *J. Chem. Phys.*, 2009, **131**, 035103.
10 B. Hernandez, F. Pfluger, A. Adenier, S. G. Kruglik and M. Ghomi, *J. Phys. Chem. B*, 2010, **114**, 15319–15330.
11 G. Y. Zhu, X. A. Zhu, Q. Fan and X. L. Wan, *Spectrochim. Acta, Part A*, 2011, **78**, 1187–1195.
12 L. Li and D. M. Lubman, *Appl. Spectrosc.*, 1988, **42**, 418–424.
13 A. E. McDermott, L. K. Thompson, C. Winkel, M. R. Farrar, S. Pelletier, J. Lugtenburg, J. Herzfeld and R. G. Griffin, *Biochemistry*, 1991, **30**, 8366–8371.
14 C. K. Teh and M. Sulkes, *J. Chem. Phys.*, 1991, **94**, 5826–5832.
15 A. Lindinger, J. P. Toennies and A. F. Vilesov, *J. Chem. Phys.*, 1999, **110**, 1429–1436.
16 R. Cohen, B. Brauer, E. Nir, L. Grace and M. S. de Vries, *J. Phys. Chem. A*, 2000, **104**, 6351–6355.
17 L. I. Grace, R. Cohen, T. M. Dunn, D. M. Lubman and M. S. de Vries, *J. Mol. Spectrosc.*, 2002, **215**, 204–219.
18 M. Zhang, Z. Huang and Z. Lin, *J. Chem. Phys.*, 2005, **122**, 134313.
19 Y. Inokuchi, Y. Kobayashi, T. Ito and T. Ebata, *J. Phys. Chem. A*, 2007, **111**, 3209–3215.
20 A. L. Maniero, V. Chis, A. Zoleo, M. Brustolon and A. Mezzetti, *J. Phys. Chem. B*, 2008, **112**, 3812–3820.
21 G. Bouchoux, S. Bourcier, V. Blanc and S. Desaphy, *J. Phys. Chem. B*, 2009, **113**, 5549–5562.
22 A. Abo-Riziq, L. Grace, B. Crews, M. P. Callahan, T. van Mourik and M. S. de Vries, *J. Phys. Chem. A*, 2011, **115**, 6077–6087.
23 K. Y. Baek, Y. Fujimura, M. Hayashi, S. H. Lin and S. K. Kim, *J. Phys. Chem. A*, 2011, **115**, 9658–9668.
24 J. R. Cable, M. J. Tubergen and D. H. Levy, *J. Am. Chem. Soc.*, 1987, **109**, 6198–6199.
25 L. C. Snoek, R. T. Kroemer, M. R. Hockridge and J. P. Simons, *Phys. Chem. Chem. Phys.*, 2001, **3**, 1819–1826.
26 L. C. Snoek, R. T. Kroemer and J. P. Simons, *Phys. Chem. Chem. Phys.*, 2002, **4**, 2130–2139.
27 H. Lioe, R. A. J. O'Hair and G. E. Reid, *J. Am. Soc. Mass Spectrom.*, 2004, **15**, 65–76.
28 D. Nolting, C. Marian and R. Weinkauf, *Phys. Chem. Chem. Phys.*, 2004, **6**, 2633–2640.
29 O. V. Boyarkin, S. R. Mercier, A. Kamariotis and T. R. Rizzo, *J. Am. Chem. Soc.*, 2006, **128**, 2816–2817.
30 K. Makara, K. Misawa, M. Miyazaki, H. Mitsuda, S.-i. Ishiuchi and M. Fujii, *J. Phys. Chem. A*, 2008, **112**, 13463–13469.
31 S. Ishiuchi, T. Asakawa, H. Mitsuda, M. Miyazaki, S. Chakraborty and M. Fujii, *J. Phys. Chem. A*, 2011, **115**, 10363–10369.
32 M. Saeki, S. Ishiuchi, M. Sakai, K. Hashimoto and M. Fujii, *J. Phys. Chem. A*, 2010, **114**, 11210–11215.
33 H. Mitsuda, M. Miyazaki, I. B. Nielsen, P. Çarçabal, C. Dedonder, C. Jouvet, S. Ishiuchi and M. Fujii, *J. Phys. Chem. Lett.*, 2010, **1**, 1130–1133.
34 S. Ishiuchi, Y. Tsuchida, O. Dopfer, K. Müller-Dethlefs and M. Fujii, *J. Phys. Chem. A*, 2007, **111**, 7569–7575.
35 S. Ishiuchi, K. Daigoku, K. Hashimoto and M. Fujii, *J. Chem. Phys.*, 2004, **120**, 3215–3220.
36 U. Even, J. Jortner, D. Noy, N. Lavie and C. Cossart-Magos, *J. Chem. Phys.*, 2000, **112**, 8068–8071.
37 Y. Okuzawa, M. Fujii and M. Ito, *Chem. Phys. Lett.*, 1990, **171**, 341–346.
38 D. Bahat, O. Cheshnovsky, U. Even, N. Lavie and Y. Magen, *J. Phys. Chem.*, 1987, **91**, 2460–2462.
39 S. E. Shamma, R. W. Amin and A. K. Shamma, *Commun. Stat. Simulat.*, 1991, **20**, 511–528.
40 H. Goto and E. Osawa, *J. Chem. Soc., Perkin Trans. 2*, 1993, 187–198.
41 H. Goto and E. Osawa, *J. Am. Chem. Soc.*, 1989, **111**, 8950–8951.
42 S. Tanabe, T. Ebata, M. Fujii and N. Mikami, *Chem. Phys. Lett.*, 1993, **215**, 347–352.
43 M. J. Frisch, G. W. Trucks, H. B. Schlegel, G. E. Scuseria, M. A. Robb, J. R. Cheeseman, G. Scalmani, V. Barone, B. Mennucci, G. A. Petersson, H. Nakatsuji, M. Caricato, X. Li, H. P. Hratchian, A. F. Izmaylov, J. Bloino, G. Zheng, J. L. Sonnenberg, M. Hada, M. Ehara, K. Toyota, R. Fukuda, J. Hasegawa, M. Ishida, T. Nakajima, Y. Honda, O. Kitao, H. Nakai, T. Vreven, J. A. Montgomery Jr., J. E. Peralta, F. Ogliaro, M. Bearpark, J. J. Heyd, E. Brothers, K. N. Kudin, V. N. Staroverov, R. Kobayashi, J. Normand, K. Raghavachari, A. Rendell, J. C. Burant, S. S. Iyengar, J. Tomasi, M. Cossi, N. Rega, J. M. Millam, M. Klene, J. E. Knox, J. B. Cross, V. Bakken, C. Adamo, J. Jaramillo, R. Gomperts, R. E. Stratmann, O. Yazyev, A. J. Austin,

R. Cammi, C. Pomelli, J. W. Ochterski, R. L. Martin, K. Morokuma, V. G. Zakrzewski, G. A. Voth, P. Salvador, J. J. Dannenberg, S. Dapprich, A. D. Daniels, Ö. Farkas, J. B. Foresman, J. V. Ortiz, J. Cioslowski and D. J. Fox, *Gaussian 09, Revision B.01*, Gaussian, Inc., Wallingford CT, 2010.

44 S. Ishiuchi, H. Mitsuda, T. Asakawa, M. Miyazaki and M. Fujii, *Phys. Chem. Chem. Phys.*, 2011, **13**, 7812–7820.

45 R. B. Gerber, G. M. Chaban, B. Brauer and Y. Miller, in *Theory and Applications of Computational Chemistry: The First Forty Years*, ed. C. E. Dykstra, G. Frenking, K. S. Kim and G. E. Scuseria, Elsevier Science, 2005, ch. 9, pp. 165–194.

46 A. G. Csaszar, C. Fabri, T. Szidarovszky, E. Matyus, T. Furtenbacher and G. Czako, *Phys. Chem. Chem. Phys.*, 2012, **14**, 1085–1106.

47 O. Christiansen, *Phys. Chem. Chem. Phys.*, 2007, **9**, 2942–2953.

48 J. M. Bowman, T. Carrington and H. D. Meyer, *Mol. Phys.*, 2008, **106**, 2145–2182.

49 D. M. Benoit, *Front. Biosci.*, 2009, **14**, 4229–4241.

50 K. Yagi, H. Karasawa, S. Hirata and K. Hirao, *ChemPhysChem*, 2009, **10**, 1442–1444.

51 G. von Helden, I. Compagnon, M. N. Blom, M. Frankowski, U. Erlekam, J. Oomens, B. Brauer, R. B. Gerber and G. Meijer, *Phys. Chem. Chem. Phys.*, 2008, **10**, 1248–1256.

52 W. Y. Sohn, M. Kim, S.-S. Kim, Y. D. Park and H. Kang, *Phys. Chem. Chem. Phys.*, 2011, **13**, 7037–7042.

53 W. Y. Sohn, K.-J. Cho, S. Y. Lee, S. S. Kang, Y. D. Park and H. Kang, *Chem. Phys. Lett.*, 2012, **525–526**, 37–43.